Scale-up of Immobilized Amine Sorbent Pellets for Landfill Gas Upgrading, using Benchtop and Pilot Equipment

Walter C. Wilfong[a,b*], Brian W. Kail[a,b], Qiuming Wang[a,b], Tuo Ji[a,b], Victor A. Kusuma[a,b], Parag Shah[c], Nicholas Fusco[c], Shouliang Yi[a,b], Fan Shi[a,b], McMahan L. Gray[a]

[a]National Energy Technology Laboratory, 626 Cochrans Mill Road, P.O. Box 10940, Pittsburgh, PA 15236-0940, USA

[b]Leidos Research Support Team, 626 Cochrans Mill Road, P.O. Box 10940, Pittsburgh, PA 15236-0940, USA

[c]PQ Corporation, Silica Catalysts, 280 Cedar Grove Road, Conshohocken, PA 19428, USA

Walter.Wilfong@netl.doe.gov*, Brian.Kail@netl.doe.gov, Qiuming.Wang@netl.doe.gov, Fan.Shi@netl.doe.gov, Tuo.Ji@netl.doe.gov, Victor.Kusuma@netl.doe.gov, Parag.Shah@pqcorp.com, Nicholas.Fusco@pqcorp.com, Shouliang.Yi@netl.doe.gov, Mac.Gray@netl.doe.gov

Highlights

- A 3.5 kg batch of immobilized amine sorbent pellet supports was commercially prepared with pilot-scale mixer-extruder equipment.
- Pellet support scale-ability primarily depended on the precursor silica/fly ash/binder solution mixture visco-elasticity, G'.
- Amine-functionalized pellets captured 1.96 mmol CO_2/g from simulated landfill gas – 35 ^oC, $CO_2/CH_4/O_2$-60/39/1.

ABSTRACT

Upgrading CO_2/CH_4 enriched biogas effluents, especially from landfills, is a viable route towards simultaneously generating renewable methane for energy production and purified carbon dioxide for industries like oil and gas, whose main use is enhanced oil recovery. Pelletized basic immobilized amine sorbents (BIAS) previously utilized for post-combustion CO_2 capture are prime candidates for CO_2 removal from landfill gas (inherent CH_4 enrichment) because of the pellets' high CO_2 selectivity and tunability for optimized performance at different temperatures and gas compositions. This work examines the process parameters and material properties that are key in the production scale-up of our previously developed polychloroprene latex-polyethylenimine (PEI, MW=25,000) binder/silica-fly ash pellet supports. Thicker pastes with aqueous binder solution/powder ratios between 2.9/1 and 3.24/1 exhibited average storage moduli of $G' \geq 9.5 \times 10^6 \pm 1.2 \times 10^5$ Pa and were easily prepared then transformed into separable cylindrical ropes via a lab-scale mixer-extruder machine. The dried supports displayed good crush strength and a >98% efficient amine impregnation. Pellets containing 32 wt% PEI_{800}/N-N-diglycidyl-4-glycidyloxyaniline crosslinker (1/0.13 wt. ratio) showed a high 1.95 mmol CO_2/g capture from simulated landfill gas (60% CO_2/39% CH_4/1% O_2) at 75 ^oC that dropped <30% after 24 hours at 105 ^oC under the same gas environment. Scalability of the material was demonstrated by producing a 3.3 kg batch of pellet supports with pilot-scale mixer and extruder equipment. Similar strength and CO_2 capture performance for the PEI-functionalized commercial pellets as those for the lab-scale pellets strongly indicate the viability of these materials for pilot-scale landfill gas CO_2 capture/upgrading.

Keywords: CO_2 capture, landfill gas, amine sorbent, pellet, scale-up, rheology

1. Introduction

Carbon capture and storage (CCS) research efforts remain widely active, especially in the "hot spot" sector of carbon capture, with over 3,500 global publications and over 4,000 citations in 2017. While the post-combustion CO_2 capture sub-category received strong attention, CCS efforts under the renewable energy sector, such as for biogas upgrading, also continued to grow.[1] Helping to bolster the growth in biogas upgrading, the U.S Environmental protection Agency established the Landfill Methane Outreach Program in 1994. This organization is comprised of industry stakeholders and waste officials and seeks to reduce or avoid CH_4 emissions from landfills, which contribute 20% of the U.S. greenhouse gas emissions.[2] Emissions from landfills can be a source of both

valuable and hazardous gases. Landfill gas (LFG) typically contains up to 45-50 vol. % CH_4, 50-55 vol. % CO_2, and 2-5 vol. % numerous chemical compounds such as N_2, sulfur oxides (SO_x), nitrogen oxides (NO_x), hydrochloric acid (HCl), and hydrogen sulfide (H_2S) generated during the anaerobic biodegradation phase of organic municipal waste.[3] Of >2,600 U.S. landfills examined, 578 currently have active remediation projects involving power generation to drive turbines, boilers, reciprocating engines, plus other equipment/devices.[4]

One key step in biogas/landfill gas upgrading is the removal of CO_2, where the gas both serves as a heat sink to reduce the energy density of the CH_4-rich gas mixture and as an unnecessary pollutant. A variety of sorbents have been developed that can adsorb CO_2 from a moderately to a highly concentrated gas stream and include (i) basic immobilized amine sorbents (BIAS) like Class 4 N-(3-(trimethoxysilyl)propyl)ethylenediamine/polyethylenimine/SiO_2[5]; (ii) porous polymers, especially metal organic frameworks (MOFs, FJU-44)[6] and benzimidazole-linked polymers (BILP, BILP-101)[7]; (iii) modified zeolites like TiO_2-5A[8]; (iv) modified carbons such as TEPA/exfoliated-graphene oxide[9]; and others. While the majority of this gas capture work emphasizes post-combustion applications, similar test protocols and reactor infrastructure for biogas upgrading as those for post-combustion remediation[10-14] make the latter endeavor ideal for these materials. Mostly physisorbents, like zeolites and activated carbon, and pressure swing reactor systems have been commercialized (Xebec, Carbotech, etc.) for biogas upgrading. However, the BIAS technology is an attractive chemisorption-based option given the high CO_2 selectivity, thermal regenerability, stability, and well-developed reactor configurations. These all can help produce consistent, highly concentrated CO_2 streams during temperature-pressure-swing desorption/regeneration cycles with minimal vacuum requirements.

Research focused towards shaping or pelletizing general sorbent particles, particularly BIAS materials, into more manageable or robust forms acknowledges the need to improve the sorbents' mechanical strength, mobility, and gas flow-through properties for pilot scale fixed bed or moving bed reactor use.[15-21] Our previous R&D efforts lead to a steam-stable (48 hours), epoxy-crosslinked BIAS pellet prepared by a scalable, latex binder-based method.[15] Scaling BIAS pellet production beyond small batches prepared by-hand (~ 5 g) to kg-scale using pelletization equipment[22, 23] is scarce and typically proceeds with an understanding of the effect that various raw material properties and production variables would have on the final dried pellet (small scale trials). One key issue with pellet scaling is establishing a viable production method that gives acceptable CO_2 capture performance and

mechanical strength. Accordingly, we prepared an array of immobilized amine sorbent pellets from our previously optimized latex polychloroprene/polyethylenimine binder plus one with polyurethane, using a commercial lab-scale pelletization machine. Herein, we examined the effect of binder solution/silica plus fly ash powder ratio (BS/P), powder particle size, and production speed on processability (rheology) of the wet binder/powder mixture, characteristics of amine impregnation (pellet support), and pellet physicochemical properties. Specifically, pellet crush strength and CO_2 capture performance in a simulated landfill gas environment were key metrics evaluated. Production of a kg-scale batch of pellet supports by our commercial partner, PQ Corporation, is the first step towards demonstrating scalability.

2. Materials and Methods

2.1 Materials

A dry mixture of amorphous silica (type CS-2129, $D_{particle,avg.}$=25 or 100 μm; PQ Corporation) and Class F Brazilian Fly Ash (FA; Beneficent Association of the Santa Catarina Coal Industry - SATC) constituted the pellet supports. Polymer binders to agglomerate the powder were polyethylenimine MW=25,000 (PEI_{25k}, Millipore Sigma) and polychloroprene latex (type 400 - PC_{400}, 47-51% solids; Showa-Denko) or polyurethane latex (Bondthane UD-301; UD_{301}, 40% solids; Bond Polymers International). A combination of polyethylenimine MW=800 (PEI_{800}) and N-N-diglycidyl-4-glycidyloxyaniline (E3, 10.8 mmol epoxide/g) epoxy crosslinker both from Millipore Sigma were used to functionalize the pellet supports. MeOH (99.0%; Fisher) served as the impregnation solvent.

2.2 Lab-scale Pellet Preparation and Functionalization

An array of BIAS pellet supports was prepared in a Caleva Multi-lab commercial pelletizer (AC Compacting) by first combining 10.0 g amounts of a FA/silica-10/90 powder (weight ratio) with binder solution in the mixing bowl accessory at binder solution/powder ratios (BS/P) between 2.7/1 and 3.6/1. The solutions were comprised of 5.4 to 7.2 wt% polymers, varied to give 16-17 wt% binder within the support, at a PEI_{25k}/latex solids weight ratio of 1/1. The binder solutions were rapidly added within 15 s to the dry powder under a mixing speed of between 8 rpm (minimum setpoint) and 40 rpm, then allowed to blend for 20 min. Twin-paddle blades set inside the mixing bowl ensured homogeneous mixtures with varying consistencies, ranging from a thin “cream” to a chunky paste. These materials were removed from the mixing bowl and gently combined by hand into a ceramic bowl for 10 to 20 s.

Next, they were gradually fed into a single-screw extruder accessory with a syringe plunger via an acrylic feed tube and extruded into 1.5 mm ropes at a machine set speed of 50 rpm. This gave a total extrusion time of $\leq$2 min. A 3-5 g portion of each extrudate was reserved and gently recombined by hand, then wrapped in parafilm prior to rheological analysis. The remaining portions of ropes were dried at 105 ^{o}C in a convection oven for 70 min, then broken by hand into 2-10 mm lengths to generate the final pellet supports.

Pellets were functionalized with a targeted 32 wt% organic loading in a 50 mL round-bottom flask by first submerging 2.0 g portions of different supports into ~21 g of impregnation solutions containing 0.96 g pure PEI_{800} (CO_2 capture screening) and E3/PEI_{800} mixtures at 0.20/1 or 0.13/1 wt. ratios (overnight stability testing) in 20 g MeOH. The flask and its contents were attached to a rotary-evaporator unit set at 50-60 ^{o}C and 15 rpm for removal of solvent, which was accomplished by stepwise pulling a vacuum from 10 to 28 in Hg over 60 min. The resulting dry functionalized pellets were removed from the flask then heated in an oven at 105 ^{o}C for 30 min to remove any residual solvent and to complete the crosslinking reaction between PEI and E3, when the tri-epoxide was present.

Residual PEI not impregnated into the supports formed a thin film on the inner wall of the flask, adhering some of the pellets. The remaining PEI was quantified by first removing the stuck pellets then rinsing the flasks with 30 mL of RO water at 40 ^{o}C. The wash solutions were subsequently diluted with water to between 1:5 and 1:25 then mixed at a 1:1 ratio with an aqueous 500 ppm $CuCl_2$ solution. The new amine-Cu mixture formed an organic-metal complex detectable by UV-Vis spectroscopy, which was used to quantify down to low ppm levels of aqueous PEI via a calibration curve of UV intensity vs. PEI concentration.[24]

2.3 Commercial Pelletization (PQ Corporation)

Silica type CS-2133 from PQ was used for commercial scale-up pellet preparation instead of type CS-2129 due to its wide commercial availability. The granular forms of these types possessed the same 2.5 cm^3/g pore volume, with CS-2133 having only 26% higher surface area and 20% lower average pore size (Table 1). The binder solution was prepared by first dissolving 293 g PEI_{25k} in 2 kg water under gentle heating on a hot plate, then adding 6,264 g water followed by 596 g PC_{400}. The 9,153 kg binder solution was incorporated into 3 kg of FA/silica-10/90 powder (lab-scale optimized BS/P=3.05), using a pilot-scale plough shear mixer. The resulting wet granules and agglomerates were transferred into a 2" single-screw extruder and passed through a 1.5 mm die at a rate of 102 g/min to form wet ropes, which were dried overnight in an oven at 90 ^{o}C to give 3.32 kg of pellet supports. Note that

the FA/CS-2133 and FA/CS-2129 powders had about the same particle size distribution and similar pre-adsorbed water contents of 3.9 and 2.4 wt%, respectively, as determined by TGA analysis.

2.4 Paste Rheology Measurements

Viscoelastic properties of the reserved, extruded pastes were measured at 23 ^{o}C with an Anton Paar Modular Compact Rheometer MCR 302 equipped with a 25 mm parallel plate accessory and a Peltier hood/plate for temperature control. The tests were carried out by amplitude sweep, using a frequency of ω=10 s^{-1} at an increasing strain of .001 to 100%. Multiple ~1.2 g amounts of the pastes were separately placed onto the sample stage and gently compressed and flattened with one finger or a spatula. The paste thickness/measurement gap was independently adjusted to between 0.8 and 1.8 mm for each test to facilitate rapid paste loading to minimize drying. After loading, 3-4 drops of water were placed outside the sample stage and the Peltier furnace hood was lowered to create a temperature controlled, humid environment. After a 10 to 13-min equilibration period, the measurement was performed, which took about 6-8 minutes. A set of 3-5 subsamples of each reserved paste was run to establish standard deviations, which account for variations arising from subsample loading and some unavoidable edge drying.

2.5 Crush Strength Measurements

Crush testing of FA/silica pellet supports and related functionalized sorbents was performed using our previously reported crush test apparatus.[15] Each of 3-5 samples from the different pellet formulations was placed horizontally beneath a vertical press rod and compressed under a gradually increasing force of 9.8 N/min until failure. Pellet crush strengths (MPa units) were calculated by dividing the crush forces by the largest cross-sections (diameter x length) and are reported here as the averages of all pellets.

2.6 Physical and Chemical Characterization

Surface and pore analyses of pellet supports were performed with a Quantachrome, Nova 2200 surface analyzer through N_2 physisorption measurements at 77 K. Prior to analyses, samples were pretreated at 110 ^{o}C under vacuum for 6-17 hours.

Diffuse reflectance FTIR (DRIFT) spectroscopy was utilized to examine the general proximity of impregnated PEI within the pellet sorbents. For this, pellets were loaded vertically side-by-side into the DRIFTS cup to expose

both their internal cross-sections and external ends to the infrared light. Cross-section scans were achieved by cutting the pellet in half with a razor and exposing the fresh surface to the IR light. While interaction of the IR beam with the lateral sides of the pellets is likely, the spectral features should be dominated by the end faces. DRIFTS spectra were obtained at 50 ^{o}C after pretreating the pellets at 120 ^{o}C under N_2 flow for 30 min then cooling down. The spectra were averaged from 100 sample scans collected over 1 min at a 4 cm^{-1} resolution.

2.7 CO_2 Capture Testing

Single-cycle CO_2 capture screening of the rod pellets was performed in a thermogravimetric analyzer (TGA) by first pre-treating the pellets at 105^{o}C for 60 min in flowing N_2 to desorb CO_2 and H_2O pre-adsorbed from the ambient atmosphere then cooling to 75 or 35^{o}C, then switching to a flow of synthetic landfill gas mixture containing either 60% CO_2/N_2 (Q500, TA Instruments, 60 mL/min) or 60% CO_2/39% CH_4/1% O_2 (ThermoCahn, ThermoFisher, 100 mL/min) for CO_2 adsorption for 30 min. A 30 min-adsorption time was enough to achieve near-equilibrium CO_2 uptake under these specific conditions. Ten CO_2 adsorption-desorption cycles of a promising pellet formulation were further performed in a TGA (TA Instruments, Q500) by adsorbing CO_2 at 35 ^{o}C from a 60% CO_2/N_2 flow for 30 min; purging gas-phase CO_2 and desorbing adsorbed CO_2 at 35 ^{o}C in N_2 flow for 10 min; then desorbing strongly adsorbed CO_2 at 105 ^{o}C in N_2 for 60 min. Standard deviation of the adsorbed CO_2 measurements for the TGA was calculated from 3 separate sing-cycle runs to be 0.027 mmol CO_2/g, showing the reliability of this experimental technique despite using <100 mg sample/run.

An overnight CO_2 capture stability test of the E3/PEI-crosslinked pellet was performed in the ThermoCahn TGA by the following method: (i) pretreating the pellets at 105 ^{o}C in 100 mL/min of flowing N_2 for 90 min to desorb the pre-adsorbed CO_2 and H_2O and cooling to 75 ^{o}C; (ii) switching the flow to the $CO_2/CH_4/O_2$ mix for 30 min for CO_2 adsorption; (iii) heating to 105 ^{o}C under the mix gas flow and holding for 24 hours for stability testing; (iv) reverting the flow back to N_2 and maintaining at 105 ^{o}C for 90 min for CO_2 desorption; (v) cooling down to 75 ^{o}C and performing a second CO_2 capture step.

3. Results and Discussion

3.1 Lab-scale Synthesis

Advancing pellet production from our previous "by-hand" [15, 25, 26] method to the pelletizer method is the first step towards scaling. Inherently, fully scaling-up demands orders-of-magnitude larger equipment, wherein complications arising from processability issues at bench-scale become magnified. Scaling mixers/granulators and extruders to achieve a desired granule or particle size, rheology, mechanical strength, etc. was typically accomplished by modeling the effect of system geometry and operating conditions on the material's physicochemical properties then performing trial-and-error experiments.[27, 28] However, time and cost constraints may be prohibitive in extensively investigating an array of system variables and material properties. Therefore, we identified FA/SiO_2/binder paste consistency as the key property to optimize at lab scale because it directly affected both the physical handling of the wet polymer/SiO_2/FA paste and the suitability of the dried pellets for functionalization.

Figure 1 shows the commercial lab-scale equipment utilized to prepare ~10 g pellet supports/batch from the mixed and extruded pastes containing different grades and particle sizes of silica and fly ash. Only room temperature studies were performed because heating the binder/powder mixture is not necessary and would raise production costs at large scale. During pelletization, quick transition from mixer to extruder accessory facilitated smooth operation and a minimal 1-2 min aging time of the powder/binder mixtures, covered in parafilm, before extrusion. Mixing and extrusion rates were controlled by adjusting the rotations-per-minute set-point of the speed dial. Binder solutions were rapidly introduced over 15 s to the powders through the feed inlet via a syringe.

Surface, pore, and particle size measurements for the particle and powder mixtures are shown in Table 1. Figure 2 shows typical flow curves for pastes prepared from 10.0 g of FA/silica (GS, D_{50}~19 µm)-10/90 mixed with 32.4 g of 6 wt% (a) PC_{400}/PEI_{25k}-1/1 and (b) UD_{301}/PEI_{25k}-1/1 binders. Our previous work confirmed that the PC_{400}-based paste formula was optimal for pellet preparation by hand, and so served as the starting point here.[15] Rheological tests were first performed through amplitude sweeps, using an ω=10 s^{-1} frequency oscillation, to identify the linear viscoelastic region (LVE). Both materials displayed viscoelastic behavior through G' (storage modulus, elasticity) >"G (loss modulus, viscosity) values. Independent of their identical LVE region from 0 to 0.000463%, drastically different yield stresses of τ_{yield}=471 and 8.2 Pa for the PC_{400}/PEI_{25k} and UD_{301}/PEI_{25k} pastes, respectively, were required to soften the materials. Moreover, τ_{flow}=4,306 and 20.6 Pa flow stresses were required to break down the pastes' structures and initiate flow.[29] These results along with overall higher G' values for the thicker PC_{400}/PEI_{25k}

paste than the thinner UD_{301}/PEI_{25k} paste indicate more energy would be required to mix and extrude the thicker PC_{400}-based mixture.

The thicker paste reflects stronger interactions imparted to the hydrated particle mixture by the -Cl of polychloroprene than by -NH(C=O)O- polyurethane. Furthermore, bulky aromatic of UD_{301} could further inhibit paste cohesion. We credit the superior adhesion of the PC_{400}-based paste to a hydrogen-bonded polymer network, wherein binder-coated [FA/silica]···PEI-PC_{400} particles are joined through interactions with a thin layer of hydrated PEI chains (-NH_2, -NH) and suspended PC_{400} nanoparticles (-Cl). We previously showed through infrared spectroscopy that PC latex-PEI-[FA/silica] interactions adhered the dried pellet supports.[15] Plotting the G"/G' [tan(δ)] versus strain fraction profiles, shown in the Supporting Information, further highlights the stronger interaction within the filler-binder network of the PEI-PC_{400} compared to the UD_{301}-PEI mixture that lead to more elastic characteristics at lower strain. However, PEI-PC_{400} gives a more brittle network than UD_{301}-PEI, as shown by the onset of G">G' (i.e. tan(δ) >1) at a lower strain fraction. So, our stronger PC_{400}-based mixture is just as readily processible as that give by the weaker UD_{301}-based binder.

Performing frequency sweep tests on both pastes at a shear strain fraction of 0.0003, which is below the yield point, enables further analysis of the materials' behavior at a relatively slower time scale (lower frequency; longer relaxion time) and faster time scale (higher frequency; shorter relaxation time) without destroying their structures.[29] Figure 2 (c) shows a slightly increasing G' profile with frequency for the PC_{400}/PEI_{25k} paste combined with consistently higher G' values than those of G". These features are consistent with those for viscoelastic aqueous alumina paste[30] and poly[styrene-co(butyl acrylate)-co-(acrylic acid)]/silica nano composite latex materials[31], highlighting the stable elastic nature of our polychloroprene-based paste. The relationship between complex viscosity (η*) and frequency (ω) , $\eta^*=(G'+iG'')/\omega$, describes the total resistance to flow contributed by the elastic and viscous portions of the paste during oscillatory tests, and can be used to evaluate shear thinning.[32] Exponentially decaying, η* profiles (normalized for easy comparison) for both PC_{400}- and UD_{301}-based pastes in Figure 2 (d) confirm shear thinning behavior. Owing to this, we predict that varying the mixing speed of the polymer binder/powder systems will alter paste consistency, and therefore processability.

Pellet supports were first prepared from FA/silica+PEI_{25k}/PC_{400} pastes mixed at different speeds (rpms), which induced varying degrees of shear thinning and gave consistencies ranging from thick agglomerates to thin "creamy"

mixtures. The qualitative consistencies of subsequently extruded and gently reshaped paste ropes were quantified by their G' values (amplitude sweep), which were categorized according to their suitability to form well-defined dried pellets. Figure 3 (a) shows that distinct ropes formed from a thick paste with "good" consistency exhibited a $G' \geq 8.6 \times 10^5$ Pa at a strain fraction of 1×10^{-5} and were smooth and minimally agglomerated after extrusion. Figure 3 (b) shows that these final dried pellets were distinctly cylindrical and easily broken into individual pellet rods. Contrastingly, paste ropes from "bad" or "poor" pastes resulting from ≥30 rpm mixing displayed $G' \leq 5.2 \times 10^5$. These G' values corresponded to sticky agglomerates, where minimal amounts of individually separated dried pellets could be obtained after drying. Although the inset images show little difference between the morphologies of the 30 rpm and 40 rpm pellets, much more of the latter than the former were discarded because they were irregular agglomerates unsuitable for impregnation and subsequent CO_2 capture. The overall G' values and viability of the pastes diminished with increased mix speed due to gradual deterioration of their elasticity. This highlights the importance of controlling shear thinning during scale-up pellet preparation.

Surprisingly irrespective of rope consistency, Figure 4 (a) shows that the mechanical strengths and CO_2 capture capacities of the dried PC_{400}/PEI_{25k}-based pellet supports and 32 wt% E3/PEI-0.20 impregnated sorbents displayed no trend. These results indicate that any appreciable effects of paste shear thinning imparted to the dried pellets, such as polymer binder orientation and location, were diminished upon drying the wet ropes. Note that some (but few) pellets suitable for crush tests were recovered from the 40 rpm-mixed extrudate given their highly agglomerated and irregular shapes. Crush strengths for the supports were all between 1.6 and 2.1 MPa, which increased to above 3.0 MPa after impregnation. This enhancement is owed to both capillary forces after filling the previously vacant pores by PEI and E3, and to amine-epoxy crosslinking that further strengthened the structure. Analysis of the pellet supports by BET surface measurements revealed a negligible effect of mix speed on the pellets' pore volume, surface area, and average pore size (data not shown). Together the results of crush testing and surface-pore analysis for the dried pellets suggests that as water is removed from the pastes during drying, regardless of consistency or degree of shear thinning, the solids and polymers reorganize into a similarly packed structure of comparable strength.

The CO_2 captured from simulated landfill gas (60% CO_2/N_2) after 30 min by all crosslinked pellet sorbents was about 1.5 mmol CO_2/g, which is consistent with different epoxy-stabilized, immobilized amine particles and pellets

for other concentrated CO_2 gas mixtures.[15, 33-35] Because overall sorbent pellet performance was unaffected by paste consistency, it is evident that precise control over paste rheology is unnecessary to achieve a viable CO_2 capture pellet if the paste ropes are separable and can form individual cylindrical pellets.

Pastes prepared from UD_{301}/PEI_{25k} binder solution were considerably soft, as characterized by excessively low G' values, and failed to produce enough separated paste ropes/dried pellets for practical application. Although the crush strength of some distinctly separate rods was found to be good, >1.3 MPa, the thin paste consistency and limited quantity of viable rods excludes these polyurethane-based pellets from further consideration. Measurably stronger crush strength of the PC_{400}/PEI_{25k}-bound solid pellets (Figure 4) and drastically higher G' values (Figure 3) of their pastes position these materials above their UD_{301}/PEI_{25k} counterparts for scale-up.

3.1.2. Effect of Powder Particle Size

Average particle size and particle size distribution are known to have a significant effect on paste rheology due to different general packing geometry, void space between larger particles, [36] and inter-particle interactions, all of which can impact the mechanical strength of the final dried pellet supports. Table 1 shows the D_{10}, D_{50}, and D_{100} values for dry mixtures prepared from fly ash and the finer, ground SiO_2 (FA/GS-10/90) and coarser, non-ground silica (FA/S_{100}-10/90). Full particle size distributions are shown in the supporting information. Both mixtures were used to prepare pellets with PC_{400} and UD_{301}-based binders. Here, D_x represents the diameter of particles comprising less than "x %" of the total sample. Values for the fly ash/silica dry powders were calculated as a volume-weighted average of the individual components. All D_x values for FA/S_{100}-10/90 were 4 to 6 times greater than those for FA/GS-10/90, endowing the latter powder with overall higher surface area (SA)/volume (V) ratios. Assuming solid spherical particles, we calculated a SA/V~0.03 μm^{-1} at D_{50} for the former mixture and a SA/V~0.16 μm^{-1} for the latter mixture. Note, V here equals skeletal volume (from pycnometer density) plus pore volume (from BET). This roughly translated to about a 5X higher capacity for the finer powder than the coarser powder to form inter-particle bonds with the polymer binder. Ineffective bonding between the coarser-particle mixture and PC_{400}/PEI_{25k} (BS/P-3.24) was glaringly evident from the thin and "creamy" texture of the overly wet extrudate associated with a 20 rpm mix speed, which led to extruded amorphous piles and rope-like ribbons. This contrasted the thick and self-supporting ropes obtained from the finer-particle powder. Comparatively, results for pastes prepared with the different-sized powders and UD_{301}/PEI_{25k} mirrored those of the PC_{400}/PEI_{25k} mixture.

Comparing the particle size distributions between the two different-sized powders, we found that the individual D_{10}/D_{50} and D_{10}/D_{100} particle size ratios were similar; 0.39 and 0.23 for FA/S_{100}-10/90 and 0.41 and 0.18 for FA/GS-10/90. These values are within the range of those found to give optimal dry packing/mechanical interlocking to a multi-sized mixture of bentonite particles (crushed pellets) having 10% of the finer particles.[37] Therefore, the packing arrangements of bound, fly ash and silica particles within each of our dried PC_{400}/PEI_{25k} and UD_{301}/PEI_{25k} pellet formulations should be similar. Owing to similar particle packing, we associate the superior crush strengths of FA/GS-based pellets over those of FA/S_{100}-based pellets, shown in Figure 5, to greater particle-binder-particle adhesion afforded through higher external surface area.

3.1.3. Effect of Solution/Powder Ratio

Pastes prepared from PC_{400}/PEI_{25k} binder and finer FA/silica powders mixed at 20 rpm were easily processed and transformed into supports suitable for impregnation. To further improve BIAS pellet production, we examined the effect of binder solution/powder ratio, BS/P, on the paste rheology and pellet mechanical strength. Figure 6 (a) shows that increasing the BS/P from 2.7 to 3.6 (27 to 36 g solution/10 g powder) linearly diminished the storage modulus and corresponding consistency of the mixture after 20 min at 20 rpm. Dryer mixtures were in the form of strongly cohesive and "lumpy" agglomerates that gave $G'=1.8 \times 10^6$ Pa for the reformed extruded ropes. By contrast, the wetter mixtures exhibited a "creamy" texture that gave $G'=1.02 \times 10^5$ Pa. We ascribe the behavior of these properties to increased wetting of the particles at higher BS/P, wherein their pore volume (23.3 mL for 10 g powder) was filled and excess solution was dispersed among their interstices.

According to granulation theory, collisions among initially formed small binder-FA/silica granules during mixing coalesced them into larger granules visible during mixing, then further consolidated them over time to increase the overall paste size. Strength of these growing paste granules depended upon their state of saturation – pendular, funicular, capillary, or droplet, and was governed by liquid binder bridge forces, capillary suction, surface tension, and interparticle friction forces.[38] Visibly wide variation in the "lump" and particle sizes of the thick BS/P 2.7 paste reflects non-uniform distribution of the binder at a calculated binder excess of 3.7 mL (ρ_{binder}~1 g/mL) relative to the 23.3 mL pore volume. Conversely, more uniform distribution of the binder for the BS/P 3.6 paste is implicated by the homogenous and smooth texture at a 12.7 mL solution excess. We propose that raising the excess binder solution shifted the proportions of funicular (under saturated), capillary (fully saturated), and droplet

(over saturated) structures in the final pastes, as shown in Figure 7. [38] Furthermore, dilution of the powder concentration at higher BS/P reduces particle-particle interactions/frictional forces. Expectedly, ropes prepared at or below the 3.24 ratio lead to dried pellet supports suitable for impregnation and CO_2 capture. The strength of the viable supports, shown in Figure 6 (b), were all between 1.9 and 2.1 MPa, whereas that for the 3.6 ratio support was drastically lower at 0.8 MPa.

3.1.4. Characterization of Amine Impregnation

Extending beyond paste processability, the extent of amine impregnation into the pellet supports is a critical consideration for scale-up. Failing to incorporate the targeted amine loading into the pellet pores would inherently produce a thin film of residual species and pellets adhered to the preparation vessel walls that requires removal. The inset image of Figure 8 highlights this issue by the ring of dried, impregnated pellet supports (20 rpm, 3.24 ratio) coating the preparation flask after attempting a 32 wt% loading of only PEI_{800}. Ultra-violet/Cu^{2+} analysis of the wash solution for this flask (30 mL H_2O, pellets removed) revealed that ~6.7 wt% of the targeted amine loading remained within the flask. This amount was similar to that left behind after impregnating the 30 rpm-mixed support, and was lower than the 10.7 wt% left behind by the 40 rpm-mixed support.

Lowering the BS/P from 3.24 to 2.9 then 2.7 gave better PEI impregnation, evidenced by the only 1.2-1.3 wt% amine remaining in the flask (98.8%, 98.7% incorporation) and lack of pellet sticking. We attribute better impregnation of the 2.7 ratio support (dryer) than the 3.24 ratio support (wetter) to uneven covering of the hydrophilic FA/SiO_2 surface with binder. We speculate that the dry mixture, resulting from an "under-mixed" paste, contained thicker inhomogeneous layers of binder scattered across the Si-OH surface of the powder. Inherently, the remaining free Si-OH served to absorb impregnated PEI_{800} via capillary action. Furthermore, agglomeration of the thicker binder layers may free-up otherwise inaccessible narrow pore space that would be covered by thinner, more homogeneously distributed layers. The lack of adhesion for the impregnated, 2.9 and 2.7 ratio pellet sorbents to the flask shows that achieving a $G' \geq 1.3 \times 10^6 \pm 1.2 \times 10^5$ Pa (8.7%) gave both an ideally processible paste and strong support that should be easily functionalized at larger scale.

Deposition of the PEI film inside the flask for the impregnated 3.24 ratio pellet reflects slower amine diffusion towards the center of the support as MeOH was evaporated compared to the other pellets. This produced a radial concentration gradient of impregnated PEI, with thicker amine layers coating the external surface. Diffuse

reflectance FTIR spectra of the impregnated pellets' cross-sectional (CS) and external end (E) surfaces and calculated IR ratios, shown in Figure 9, suggest this gradient from the different infrared ratios of PEI (1460 cm^{-1}, C-H stretch)/silica (808 cm^{-1}, Si-O-Si stretch; bulk structure internal standard).[39] Ratioing the 1460/808 band intensities qualifies the amount of impregnated PEI against an internal standard unaffected by impregnation. An increasing $E_{1460/808}$ value with binder solution/powder ratio reflects accumulation of amine at the pellet's exterior that lead to sticking on the flask. SEM-EDS elemental analysis of the external, lateral surface of the 3.24 and 2.7 ratio pellets confirm the IR results, showing a higher N/Si ratio of 0.34 for the former and lower 0.29 ratio for the latter. An apparent radial concentration gradient of amine was indicated for only the 3.24 BS/P pellet by the ratio of external/internal amine layers, $E_{1460/808}/CS_{1480/808}$= 1.24, compared to <1 for the other pellets. However, the elemental analysis revealed higher N (PEI_{25k} and PEI_{800})/Si and Cl (PC_{400})/Si ratios for the internal cross-sections than for the lateral surfaces of both pellets (Table S1 in the SI). This suggests, in part, slightly higher binder content distributed inside the pellet, and conflicts the amine gradient implied by DRIFTS. Despite this discrepancy, excess amine on the external surface of the BS/P-3.24 pellet was confirmed. This external amine surface layer would be unstable during steam-induced CO_2 desorption at higher temperatures, as suggested elsewhere [5], and could diminish the CO_2 adsorption kinetics at temperatures lower than 75 ^oC – a known optimum for PEI/silica sorbents.

Figure 10 (a)-(c) show the CO_2 adsorption profiles at 35 and 75 ^oC for the BS/P-2.7, 2.9, and 3.24 pellet sorbents containing 30-32 wt% PEI. Gradual uptake of CO_2 by all sorbents at 75 ^oC coupled with higher total capacity after ~30 min was contrasted by faster kinetics but lower capacity at 35 ^oC. Adsorbing at higher temperature facilitated gradual CO_2 diffusion into the pores as PEI viscosity was reduced, allowing access to more amine sites after reaching near-equilibrium compared to accessing fewer sites at lower temperature.[40] Lowering the adsorption temperature inhibited CO_2 diffusion through more viscous PEI layers. Similar sensitivity of CO_2 capture towards temperature was observed for PEI-functionalized MCM-41 and SBA-15 particles and pellets.[40-43] CO_2 adsorption rate profiles, shown in Figure 10 (d-f), highlight the diffusion limitations at lower temperature from the trailing in mmol CO_2/g*min values between 3 and 8 min, i.e. asymmetric profile features about the time of the peak rate.[40, 44] The profiles further distinguish the key effects of BS/P ratio on the CO_2 uptake performance of the PEI-functionalized sorbent pellets. High concentration of available amines within the thick PEI film covering the pores of the 3.24 ratio sorbent contributed to a slightly faster maximum CO_2 uptake rate of 1.58 mmol CO_2/g*min at 75 ^oC compared to that of 1.26 mmol CO_2/g*min for the 2.7 ratio sorbent. Contrasting this at 35 ^oC, the viscous film

provided a barrier to CO_2 mass transfer and gave the 3.24 ratio pellet 36% slower adsorption kinetics, 1.59 mmol CO_2/g*min, relative to 2.5 mmol CO_2/g*min for the non-coated 2.7 ratio pellet. Higher total CO_2 capture capacity and faster kinetics at 75 ^oC for the 2.9 ratio sorbent than for the 2.7 ratio sorbent situate this material better for hotter adsorption conditions. Although 35 ^oC adsorption showed higher uptake capacity for the former, the latter displayed appreciably faster kinetics. This is important in fixed bed applications, where capture capacity up to breakthrough is more important than maximum capacity.

Stability testing of a 32 wt% E3/PEI-0.13 pellet with the optimal support (20 rpm, BS/P-2.9) was performed by exposing the pellet to the dry 60% CO_2/39%CH_4/1% O_2 at 105 ^oC for 24 hours to assess the viability for practical landfill gas treatment. This formulation was chosen for its higher capacity compared to the E3/PEI-0.20 sorbent pellet and its previously successful post-combustion CO_2 capture, involving 14% CO_2/He in our previous work.[15]

Results shown in Figure 11 reveal a moderate 28.6% loss in capacity, from 1.96 to 1.4 mmol CO_2/g after thermal treatment. We attribute this primarily to oxidation of amines to deactivated amide species and to urea formation through irreversible reaction of PEI with CO_2.[45] The loss in capacity here resembles the 25% loss of a PEI_{800}/SBA-15 particle sorbent after 10 hr exposure to 5% CO_2/N_2 and the 37% loss after 30 hr exposure to $CO_2/O_2/N_2$-5/14/81 at 100-105 ^oC.[46] Although degradation here seems excessive, the presence of water vapor in real landfill gas streams will dramatically reduce urea formation and sorbent degradation.[47] Addition of an antioxidant, like K_2CO_3 or Na_2CO_3, could further inhibit degradation by minimizing amine oxidation.[15, 48]

3.2 Validation of Commercial Pellets

The recent lack of commercially available quantities of CS-2129 silica predicated the need to use the readily available CS-2133, which exhibited similar properties as CS-2129. Preliminary lab-scale trials with a fly ash/CS-2133 silica-10/90 dry powder yielded an optimum binder solution/powder ratio of 3.05 under 20 rpm of mixing, where the resulting paste chunks exhibited an average G'= $1.1x10^6$ Pa ($\pm 5.0x10^4$ Pa, 4.5%). Results for the material commercially pelletized by PQ Corp. are shown in Figure 12, where (a) reveals that rather than a paste, a collection of different-sized wet granules was achieved with a plough shear mixer. Granules suggest a relatively low degree of shear mixing compared to the relatively high shear mixing of the lab-scale twin-paddled mixer that formed a paste. Unfortunately, the visco-elastic properties of the granules could not be measured due to the ambiguous change in their properties during sample shipment from PQ to NETL. However, we expect the G' value for this mixture

(BS/P-3.05) to be greater than the 1.0-1.2x10^6 Pa range exhibited by lab-scale CS-2129-based mixtures prepared with BS/P ratios of 2.9-3.24 (Figure 6) and for the lab-scale CS-2133-based mixture. Ideally, wet granules (high G') are superior over a sticky paste (low G') for scaleup pelletization because they eliminate the need for time-consuming, laborious scraping of a paste from the plough share mixer.

The CO_2 capture profiles in Figure 12 (b) highlight alternately higher uptake capacity and faster maximum uptake rate at 75 °C (2.27 mmol CO_2/g, 2.1 mmol CO_2/g·min) and 35 °C (1.93 mmol CO_2/g, 2.5 mmol CO_2/g·min) respectively, similarly as observed for the lab-scale CS-2129-based pellets. Slight improvement in the maximum uptake kinetics for this commercial CS-2133-based pellet at 75 °C, ~30%, compared to the lab-scale CS-2129-based pellet (Figure 10) is owed to the somewhat dryer consistency of the precursor granules. Meaning, less binder among the particle interstices gave better incorporation of impregnated amines within the commercial pellets. Effective lab-scale PEI impregnation, 99.1% of target, was confirmed by the only 0.9 wt% of target PEI remaining in the flask. Crush testing confirmed that the mechanical strengths of the support, 2 MPa ±17%, and PEI-impregnated sorbents, ~2.8 MPa ±6%, were close to those of their lab-scale counterparts.

Figure 13 shows results from cycle testing of the commercial pellet supports functionalized with a nominal 32 wt% E3/PEI-0.13, where CO_2 was adsorbed for 30 min at 35 °C from 60% CO_2/N_2 then fully desorbed at 105 °C in N_2 for 30 min. Following only a slight initial drop in CO_2 capture capacity from cycle 1 to 2, <0.1 mmol CO_2/g, the capacity remained essentially stable around 1.2 mmol CO_2/g up through cycle 10. EDS analysis of the external surface of the fresh and cycled pellets showed a 13.5% drop in the N/Si ratio. This indicates that the evaporation of non-crosslinked species was largely responsible for the loss in CO_2 capture capacity. Overall, successful scale-up of BIAS pellet supports using pilot-scale equipment shows promise for practical CO_2 capture applications.

4. Conclusions

Investigation of the key factors affecting the scale-up of basic immobilized amine sorbent pellet supports revealed that the visco-elasticity of the precursor silica/fly ash/polyethylenimine-polychloroprene binder mixture determines the paste processability and affects the degree of amine functionalization of the dried pellet support. Excessively mixed/shear-thinned pastes lacked the cohesion to form self-supporting ropes and dried rods, and yielded insufficient amine-impregnation that caused pellets to adhere to the preparation flask. Ideal pastes/granules exhibited a G' value >1x10^6 Pa, facilitating scale-up to >3 kg using commercial pilot-scale equipment. A CO_2

capture of 2.27 mmol CO_2/g from simulated landfill gas and crush strength of 2.8 MPa for impregnated (at lab scale), commercially prepared pellet supports demonstrates a good first step towards pilot-scale synthesis and testing at ≥100 kg scale for biogas applications. Further work would involve impregnation of the 3.3 kg batch pellet supports with a commercial double-cone vacuum dryer.

Declaration of Competing Interests

The authors declare no competing financial interest involved with this specific work. The authors do declare a licensing agreement between NETL and PQ Corporation for other particle sorbent technology used for aqueous metal uptake.

Disclaimer

This project was funded by the United States Department of Energy, National Energy Technology Laboratory, in part, through a site support contract. Neither the United States Government nor any agency thereof, nor any of their employees, nor the support contractor, nor any of their employees, makes any warranty, express or implied, or assumes any legal liability or responsibility for the accuracy, completeness, or usefulness of any information, apparatus, product, or process disclosed, or represents that its use would not infringe privately owned rights. Reference herein to any specific commercial product, process, or service by trade name, trademark, manufacturer, or otherwise does not necessarily constitute or imply its endorsement, recommendation, or favoring by the United States Government or any agency thereof. The views and opinions of authors expressed herein do not necessarily state or reflect those of the United States Government or any agency thereof.

References

[1] H. Li, H.-D. Jiang, B. Yang, H. Liao, An analysis of research hotspots and modeling techniques on carbon capture and storage, Science of the total environment, 687 (2019) 687-701.

[2] L. Aepli, United States Environmental Protection Agency, Encouraging the recovery and beneficial use of biogas generated from municipal solid waste, SWANA Old Dominion Chapter Conference [PowerPoint slides], 2017, web: https://www.epa.gov/sites/production/files/2017-09/documents/lmop_virginia_april2017_aepli.pdf, accessed: December 2020.

[3] United States Environmental Protection Agency, Landfill Methane Outreach Program (LMOP), Landfill Gas Energy Project Development Handbook - Chapter 1. Landfill Gas Energy basics, 2017, web: https://www.epa.gov/lmop/landfill-gas-energy-project-development-handbook-files, accessed: December 2020.

[4] United States Environmental Protection Agency, Landfill Methane Outreach Program (LMOP), Project and Landfill Data by State, 2020, web: https://www.epa.gov/lmop/project-and-landfill-data-state, acessed: December 202.

[5] W.C. Wilfong, B.W. Kail, C.W. Jones, C. Pacheco, M.L. Gray, Spectroscopic Investigation of the Mechanisms Responsible for the Superior Stability of Hybrid Class 1/Class 2 CO_2 Sorbents: A New Class 4 Category, ACS Applied Materials & Interfaces, 8 (2016) 12780-12791.

[6] Y. Ye, H. Zhang, L. Chen, S. Chen, Q. Lin, F. Wei, Z. Zhang, S. Xiang, Metal–Organic Framework with Rich Accessible Nitrogen Sites for Highly Efficient CO_2 Capture and Separation, Inorganic Chemistry, 58 (2019) 7754-7759.

[7] A.K. Sekizkardes, J.T. Culp, T. Islamoglu, A. Marti, D. Hopkinson, C. Myers, H.M. El-Kaderi, H.B. Nulwala, An ultra-microporous organic polymer for high performance carbon dioxide capture and separation, Chemical Communications, 51 (2015) 13393-13396.

[8] Z. Song, Q. Dong, W.L. Xu, F. Zhou, X. Liang, M. Yu, Molecular Layer Deposition-Modified 5A Zeolite for Highly Efficient CO_2 Capture, ACS Applied Materials & Interfaces, 10 (2018) 769-775.

[9] S. Gadipelli, Y. Lu, N.T. Skipper, T. Yildirim, Z. Guo, Design of hyperporous graphene networks and their application in solid-amine based carbon capture systems, Journal of Materials Chemistry A, 5 (2017) 17833-17840.

[10] M.J. Bos, V. Kroeze, S. Sutanto, D.W.F. Brilman, Evaluating Regeneration Options of Solid Amine Sorbent for CO_2 Removal, Industrial & Engineering Chemistry Research, 57 (2018) 11141-11153.

[11] L. Bisone, S. Bittanti, S. Canevese, A. De Marco, V. Prandoni, Cyclic Automation of a Plant for the Removal of CO_2 from Biogas, IFAC-PapersOnLine, 50 (2017) 10802-10807.

[12] S. Sutanto, J.W. Dijkstra, J.A.Z. Pieterse, J. Boon, P. Hauwert, D.W.F. Brilman, CO_2 removal from biogas with supported amine sorbents: First technical evaluation based on experimental data, Separation and Purification Technology, 184 (2017) 12-25.

[13] W. Jung, J. Park, K.S. Lee, Moving bed adsorption process based on a PEI-silica sorbent for CO_2 capture, International Journal of Greenhouse Gas Control, 67 (2017) 10-19.

[14] L. Bisone, S. Bittanti, S.M. Canevese, A. De Marco, S. Garatti, M. Notaro, V. Prandoni, A Postcombustion Carbon Capture Process by Amines Supported on Solid Pellets with Estimation of Kinetic Parameters, Industrial & Engineering Chemistry Research, 54 (2015) 2743-2762.

[15] W.C. Wilfong, B.W. Kail, B.H. Howard, Q. Wang, F. Shi, T. Ji, M.L. Gray, Steam-Stable Basic Immobilized Amine Sorbent Pellets for CO_2 Capture Under Practical Conditions, ACS Applied Materials & Interfaces, 11 (2019) 38336-38346.

[16] A.H. Valekar, K.-H. Cho, U.H. Lee, J.S. Lee, J.W. Yoon, Y.K. Hwang, S.G. Lee, S.J. Cho, J.-S. Chang, Shaping of porous metal–organic framework granules using mesoporous ρ-alumina as a binder, RSC Advances, 7 (2017) 55767-55777.

[17] G.P. Knowles, Z. Liang, A.L. Chaffee, Shaped polyethyleneimine sorbents for CO_2 capture, Microporous and Mesoporous Materials, 238 (2017) 14-18.

[18] V. Finsy, L. Ma, L. Alaerts, D.E. De Vos, G.V. Baron, J.F.M. Denayer, Separation of CO_2/CH_4 mixtures with the MIL-53(Al) metal–organic framework, Microporous and Mesoporous Materials, 120 (2009) 221-227.

[19] W. Klinthong, C.-H. Huang, C.-S. Tan, Polyallylamine and NaOH as a novel binder to pelletize amine-functionalized mesoporous silicas for CO_2 capture, Microporous and Mesoporous Materials, 197 (2014) 278-287.

[20] H. Thakkar, S. Eastman, A. Al-Mamoori, A. Hajari, A.A. Rownaghi, F. Rezaei, Formulation of Aminosilica Adsorbents into 3D-Printed Monoliths and Evaluation of Their CO_2 Capture Performance, ACS Applied Materials & Interfaces, 9 (2017) 7489-7498.

[21] F. Rezaei, M.A. Sakwa-Novak, S. Bali, D.M. Duncanson, C.W. Jones, Shaping amine-based solid CO_2 adsorbents: Effects of pelletization pressure on the physical and chemical properties, Microporous and Mesoporous Materials, 204 (2015) 34-42.

[22] R. Begag. Bench Scale Development and Testing of Aerogel Sorbents for CO_2 Capture Final Technical Report. Report DOE-FE-13172. United States. DOI: 10.2172/1349123, 2017, web: https://www.osti.gov/servlets/purl/13491232018, accessed: Nov. 31, 2018

[23] M. Isenberg, S.S.C. Chuang, The Nature of Adsorbed CO_2 and Amine Sites on the Immobilized Amine Sorbents Regenerated by Industrial Boiler Steam, Industrial & Engineering Chemistry Research, 52 (2013) 12530-12539.

[24] W.C. Wilfong, B.W. Kail, Q. Wang, M.L. Gray, Novel Rapid Screening of Basic Immobilized Amine Sorbent/Catalyst Water Stability by a UV/Vis/Cu^{2+} Technique, ChemSusChem, 11 (2018) 4114-4122.

[25] W.C. Wilfong, M.L. Gray, B.W. Kail, B.H. Howard, Pelletization of Immobilized Amine Carbon Dioxide Sorbents with Fly Ash and Poly(vinyl chloride), Energy Technology, 4 (2016) 610-619.

[26] W.C. Wilfong, B.W. Kail, B.H. Howard, T. Fernandes de Aquino, S. Teixeira Estevam, M.L. Gray, Robust Immobilized Amine CO_2 Sorbent Pellets Utilizing a Poly(Chloroprene) Polymer Binder and Fly Ash Additive, Energy Technology, 5 (2017) 228-233.

[27] T.M. Chitu, D. Oulahna, M. Hemati, Wet granulation in laboratory scale high shear mixers: Effect of binder properties, Powder Technology, 206 (2011) 25-33.

[28] J.A. Covas, A. Gaspar-Cunha, Extrusion Scale-up: An Optimization-based Methodology, International Polymer Processing, 24 (2009) 67-82.

[29] Mazger T.G, Applied Rheology: With Joe Flow on Rheology Road, 5th ed., Anton Paar, Graz, Austria, 2018.

[30] H. Liu, Y. Li, D. Li, Research on rheological properties and extrusion behavior of aqueous alumina paste in paste-extrusion-based SFF processes, The International Journal of Advanced Manufacturing Technology, 83 (2016) 2039-2047.

[31] B. You, N. Wen, Y. Cao, S. Zhou, L. Wu, Preparation and properties of poly [styrene-co-(butyl acrylate)-co-(acrylic acid)]/silica nanocomposite latex prepared using an acidic silica sol, Polymer international, 58 (2009) 519-529.

[32] Malvern Instruments, A Basic Introduction to Rheology (White Paper), Worcestershire, UK, 2016, web: https://cdn.technologynetworks.com/TN/Resources/PDF/WP160620BasicIntroRheology.pdf, accessed: Oct. 2020.

[33] S. Park, K. Choi, H.J. Yu, Y.-J. Won, C. Kim, M. Choi, S.-H. Cho, J.-H. Lee, S.Y. Lee, J.S. Lee, Thermal stability enhanced tetraethylenepentamine/silica adsorbents for high performance CO_2 capture, Industrial & Engineering Chemistry Research, 57 (2018) 4632-4639.

[34] K. Min, W. Choi, C. Kim, M. Choi, Oxidation-stable amine-containing adsorbents for carbon dioxide capture, Nature communications, 9 (2018) 1-7.

[35] H. Jung, S. Jeon, D.H. Jo, J. Huh, S.H. Kim, Effect of crosslinking on the CO_2 adsorption of polyethyleneimine-impregnated sorbents, Chemical Engineering Journal, 307 (2017) 836-844.

[36] S. Olhero, J. Ferreira, Influence of particle size distribution on rheology and particle packing of silica-based suspensions, Powder Technology, 139 (2004) 69-75.

[37] Z.-R. Liu, W.-M. Ye, Z. Zhang, Q. Wang, Y.-G. Chen, Y.-J. Cui, Particle size ratio and distribution effects on packing behaviour of crushed GMZ bentonite pellets, Powder Technology, 351 (2019) 92-101.

[38] S.M. Iveson, J.D. Litster, K. Hapgood, B.J. Ennis, Nucleation, growth and breakage phenomena in agitated wet granulation processes: a review, Powder technology, 117 (2001) 3-39.

[39] U. Tumuluri, M. Isenberg, C.-S. Tan, S.S.C. Chuang, In Situ Infrared Study of the Effect of Amine Density on the Nature of Adsorbed CO_2 on Amine-Functionalized Solid Sorbents, Langmuir, 30 (2014) 7405-7413.

[40] X. Wang, V. Schwartz, J.C. Clark, X. Ma, S.H. Overbury, X. Xu, C. Song, Infrared Study of CO_2 Sorption over "Molecular Basket" Sorbent Consisting of Polyethylenimine-Modified Mesoporous Molecular Sieve, The Journal of Physical Chemistry C, 113 (2009) 7260-7268.

[41] N. Gargiulo, A. Peluso, P. Aprea, F. Pepe, D. Caputo, CO_2 adsorption on polyethylenimine-functionalized SBA-15 mesoporous silica: isotherms and modeling, Journal of chemical & engineering data, 59 (2014) 896-902.

[42] W. Klinthong, C.-H. Huang, C.-S. Tan, One-pot synthesis and pelletizing of polyethylenimine-containing mesoporous silica powders for CO_2 capture, Industrial & Engineering Chemistry Research, 55 (2016) 6481-6491.

[43] P. Sharma, J.-K. Seong, Y.-H. Jung, S.-H. Choi, S.-D. Park, Y.I. Yoon, I.-H. Baek, Amine modified and pelletized mesoporous materials: Synthesis, textural–mechanical characterization and application in adsorptive separation of carbondioxide, Powder technology, 219 (2012) 86-98.

[44] R. Sanz, G. Calleja, A. Arencibia, E.S. Sanz-Pérez, CO_2 Uptake and Adsorption Kinetics of Pore-Expanded SBA-15 Double-Functionalized with Amino Groups, Energy & Fuels, 27 (2013) 7637-7644.

[45] C.S. Srikanth, S.S.C. Chuang, Spectroscopic Investigation into Oxidative Degradation of Silica-Supported Amine Sorbents for CO_2 Capture, ChemSusChem, 5 (2012) 1435-1442.

[46] A. Heydari-Gorji, A. Sayari, Thermal, Oxidative, and CO_2-Induced Degradation of Supported Polyethylenimine Adsorbents, Industrial & Engineering Chemistry Research, 51 (2012) 6887-6894.

[47] A. Sayari, Y. Belmabkhout, Stabilization of Amine-Containing CO_2 Adsorbents: Dramatic Effect of Water Vapor, Journal of the American Chemical Society, 132 (2010) 6312-6314.

[48] W.C. Wilfong, In Situ FTIR and Tubular Reactor Studies For CO_2 Capture of Immobilized Amine Sorbents and Liquid Amine Films, Dissertation, Department of Chemical and Biomolecular Engineering, The University of Akron: Akron, OH, 2014. Ohiolink. web: https://etd.ohiolink.edu/apexprod/rws_olink/r/1501/10?p10_etd_subid=96388&clear=10, accessed: Aug. 2014.

Figure 1: Caleva Multi Lab pelletizer used to prepare lab-scale batches of pellet supports.

Figure 2: Typical behavior of flow curves during amplitude sweep tests for extruded and recombined paste ropes, comprising a mixture of 32.4 g of 6 wt% (a) PC_{400}/PEI_{25k}-1/1 and (b) UD_{301}/PEI_{25k}-1/1 binder solution and 10.0 g of FA/silica (GS, D_{50}=19)-10/90 powder; mixed at 20 rpm. Frequency sweep tests at 0.0003 strain fraction, showing effects on (c) G' and G" and (d) normalized complex viscosity, η^*.

Figure 3: (a) Quantification of the effect of mixing speed on the consistency and processability of BIAS pastes through storage modulus (G') measurements. The binder solution contained 6 wt% PC_{400}/PEI_{25k} and the binder solution/FA+silica powder ratio, BS/P, was 3.24. (b) Resulting dried pellet supports prepared from pastes processed with different mixing speeds. Measurements were taken of the reformed, extruded ropes.

Figure 4: (a) Relationship between pellet crush strength plus CO_2 capture capacity (60% CO_2/N_2) and the processability (storage modulus, G') of paste ropes from which the PC_{400}/PEI_{25k}-based supports and impregnated sorbents were prepared. The inset values overlapping the bars represent the speed (rpms) at which the associated pastes were mixed. Effect of mix speed on the (b) storage modulus and (c) crush strength of UD_{301}/PEI_{25k}-based pellet supports.

Figure 5: Effect of fly ash/silica particle size on the mechanical strength of pellet supports prepared with PC_{400}/PEI_{25k} and UD_{301}/PEI_{25k} polymer binders.

Figure 6: Effect of PC_{400}/PEI_{25k} binder solution/powder (FA/silica) ratio, BS/P, on (a) paste consistency/storage modulus and (b) dried pellet support mechanical strength. Pastes (and pellets) were prepared with a mix speed of 20 rpm.

Figure 7: Hypothesized states of saturation of fly ash/silica powder by polyethylenimine/polychloroprene/water binder solution

Figure 8: Effect of paste mix speed and binder solution/powder ratio on the effective impregnation of PEI_{800} into corresponding pellet supports. The wt% PEI remaining in the flask is calculated by dividing the amount of PEI found in the wash solution (UV-Vis/Cu^{2+} analysis) by the 0.96 g of PEI targeted for impregnation into 2.0 g of pellet supports.

Figure 9: (a) Relative distribution of impregnated PEI_{800} on the internal and external surfaces of the 20 rpm-prepared pellet sorbents, as qualified by diffuse reflectance infrared Fourier transform spectroscopy (DRIFTS). Spectra were obtained at 50 °C after pretreating at 120 °C under N_2 flow for 30 min then cooling down. The black and red dotted lines represent spectral baselines. Absorbance=log(1/I), where I is the single beam spectrum of each pretreated sample. (b) IR absorbance intensity ratios calculated from (a).

Figure 10: Transient TGA profiles for (a-c) CO_2 adsorption amount and (d-f) CO_2 adsorption rate (ΔCO_2 Ads./Δt) for 30-32 wt% PEI_{800}-impregnated supports (20 rpm; BS/P-2.7, 2.9, 3.24) under simulated landfill gas conditions – 60% CO_2/39% CH_4/1% O_2 at 35 and 75 ^oC. The inset numbers in (a-c) represent the total mmol CO_2/g capture capacity of the pellets after ~30 min of adsorption. The inset images in (d-f) illustrate the hypothetical PEI_{800} (red) pore filling motifs.

Figure 11: CO_2 adsorption profiles for a 32 wt% E3/PEI-0.13/1 pellet sorbent (20 rpm, BS/P-2.9), both fresh and after 24 hr degradation testing in the simulated landfill gas at 105 ^oC

Figure 12: (a) Commercially prepared wet granules formed by a plough share mixer and pellet supports after extruding from a single-screw extruder and drying at 90ºC. Transient TGA weight profiles for the cumulative uptake of CO_2 (b, top) and the rate of CO_2 uptake (b, bottom) by commercial pellet supports impregnated with PEI, using the lab-scale rotary-evaporator. The inset numbers in (b) represent the total mmol CO_2/g capture capacity of the pellets after ~30 min of adsorption.

Figure 13: CO_2 capture cycling results for commercially prepared pellets functionalized at lab scale with E3/PEI-0.13. The inset table shows the elemental composition (EDS, wt%) of key species on the external pellet surfce before and after testing.

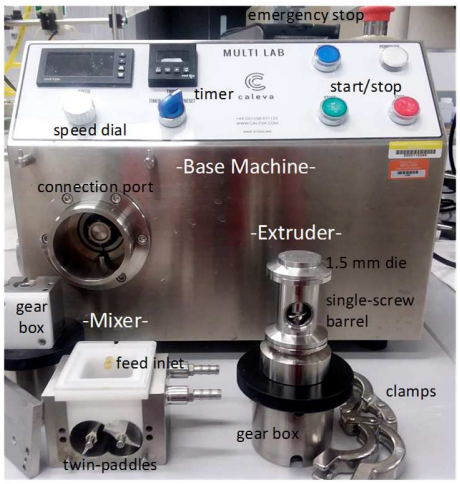
emergency stop
MULTI LAB
timer
caleva
start/stop
speed dial
-Base Machine-
connection port
-Extruder-
1.5 mm die
single-screw
barrel
gear
box
-Mixer-
feed inlet
clamps
gear box
twin-paddles

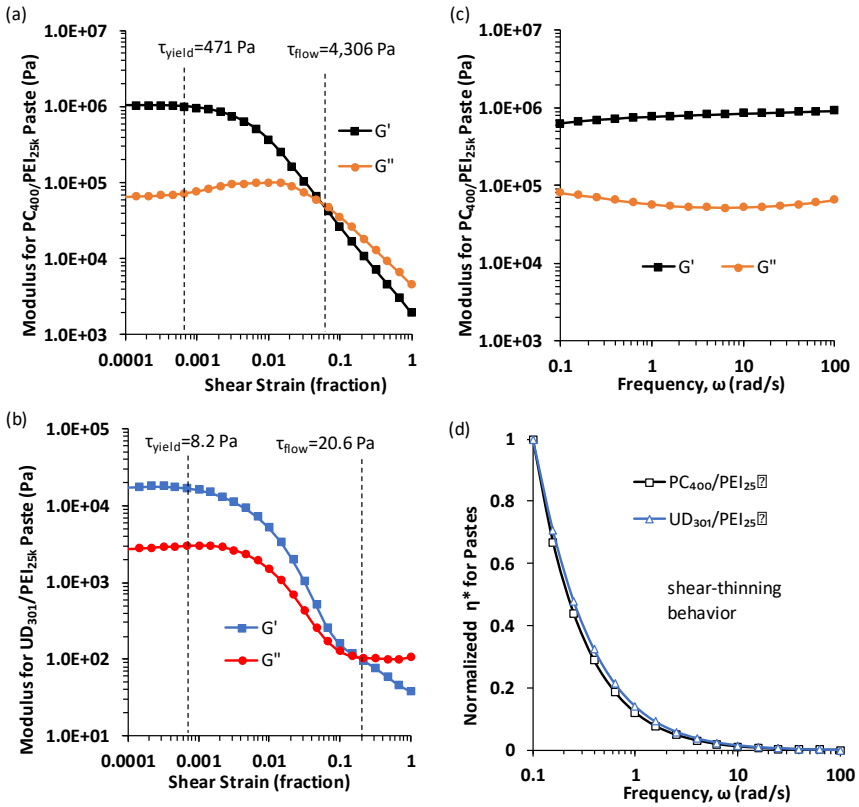
(a)
τyield=471 Pa
τflow=4,306 Pa
G'
G"
Modulus for PC400/PEI25k Paste (Pa)
Shear Strain (fraction)
(b)
τyield=8.2 Pa
τflow=20.6 Pa
Modulus for UD301/PEI25k Paste (Pa)
(c)
Frequency, ω (rad/s)
(d)
PC400/PEI25
UD301/PEI25
shear-thinning behavior
Normalizedd η* for Pastes

(a)

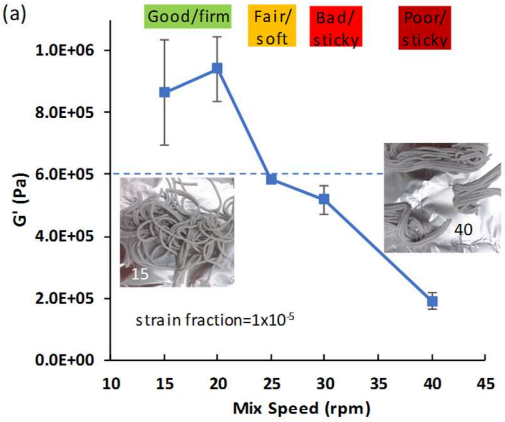

(b)

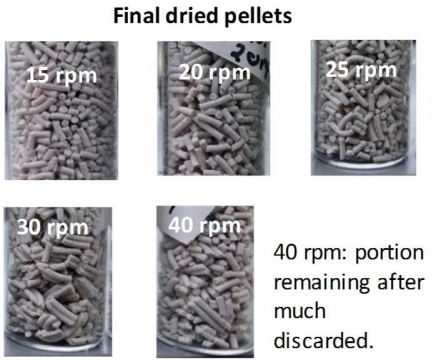

40 rpm: portion remaining after much discarded.

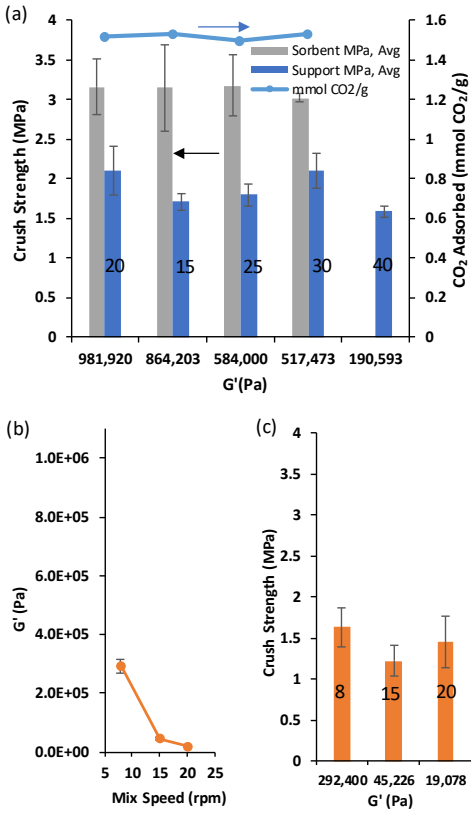
(a)
Sorbent MPa, Avg
Support MPa, Avg
mmol CO2/g
Crush Strength (MPa)
CO2 Adsorbed (mmol CO2/g)
20
15
25
30
40
981,920
864,203
584,000
517,473
190,593
G'(Pa)
(b)
G' (Pa)
Mix Speed (rpm)
(c)
Crush Strength (MPa)
8
15
20
292,400
45,226
19,078
G' (Pa)

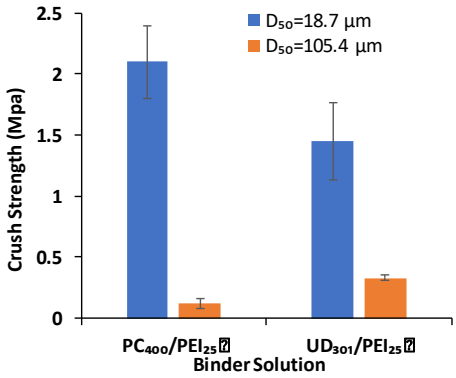
2.5
2
1.5
1
0.5
0
Crush Strength (Mpa)
D50=18.7 µm
D50=105.4 µm
PC400/PEI25
UD301/PEI25
Binder Solution

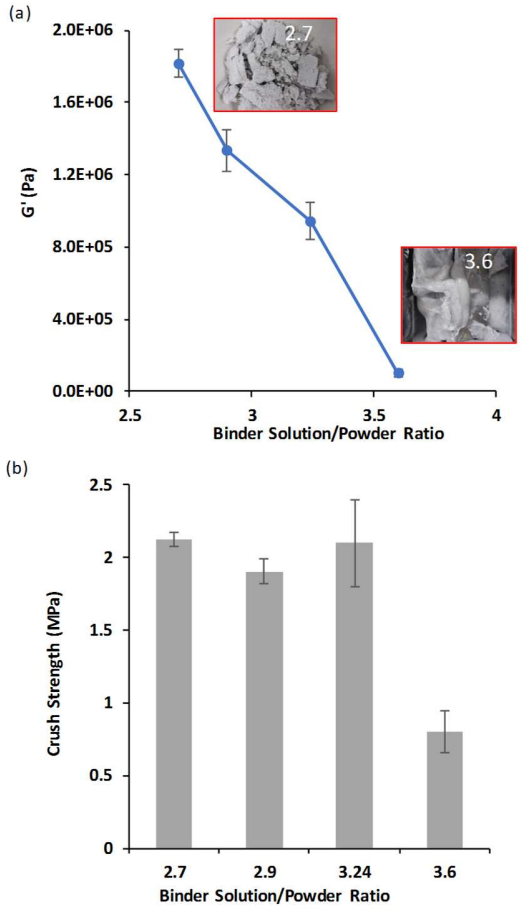
(a)
2.0E+06
1.6E+06
1.2E+06
8.0E+05
4.0E+05
0.0E+00
G' (Pa)
2.7
3.6
2.5
3
3.5
4
Binder Solution/Powder Ratio
(b)
2.5
2
1.5
1
0.5
0
Crush Strength (MPa)
2.7
2.9
3.24
3.6
Binder Solution/Powder Ratio

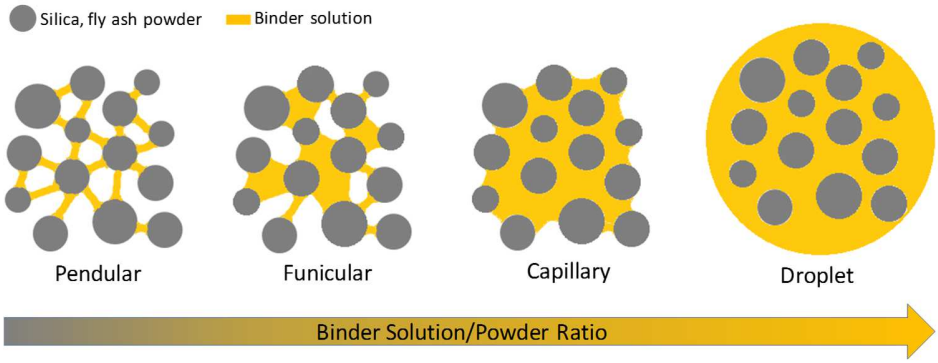
Silica, fly ash powder
Binder solution
Pendular
Funicular
Capillary
Droplet
Binder Solution/Powder Ratio

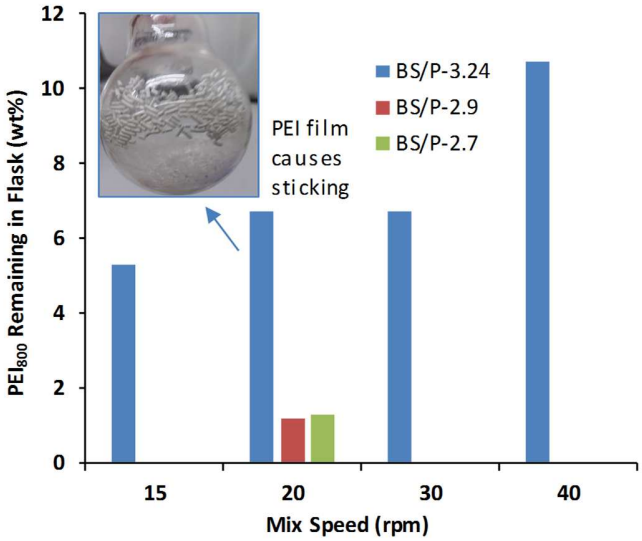
12
10
8
6
4
2
0
PEI800 Remaining in Flask (wt%)
PEI film causes sticking
BS/P-3.24
BS/P-2.9
BS/P-2.7
15
20
30
40
Mix Speed (rpm)

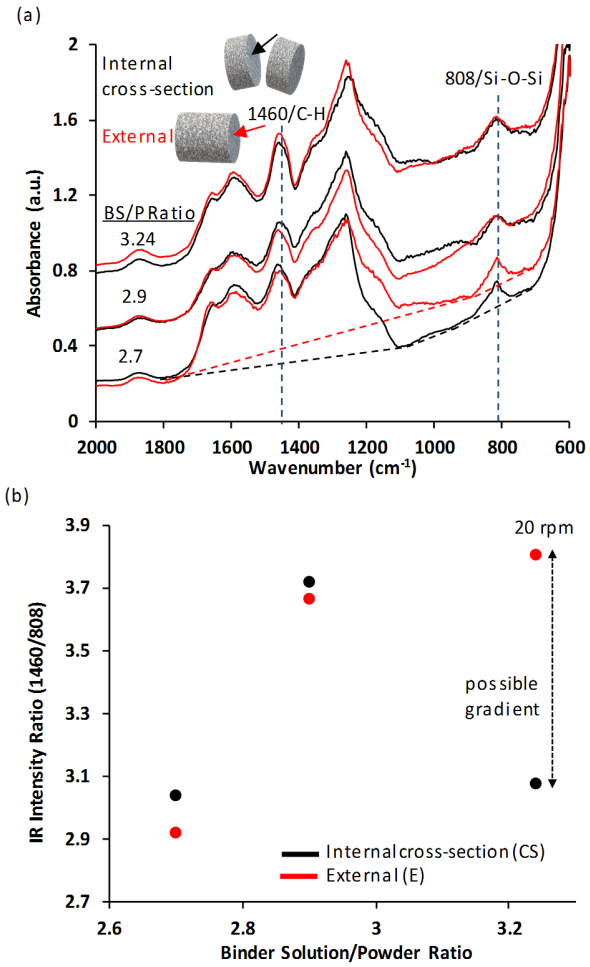
(a)
Internal
cross-section
External
1460/C-H
808/Si-O-Si
BS/P Ratio
3.24
2.9
2.7
Absorbance (a.u.)
Wavenumber (cm-1)
(b)
20 rpm
possible
gradient
Internal cross-section (CS)
External (E)
IR Intensity Ratio (1460/808)
Binder Solution/Powder Ratio

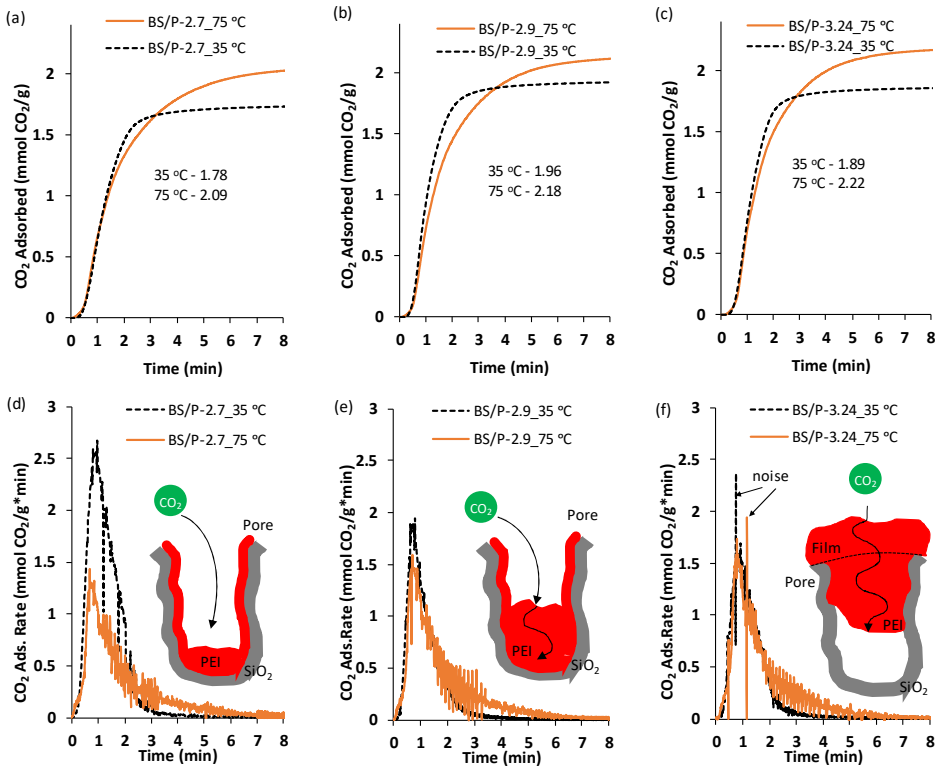
(a)
BS/P-2.7_75 ºC
BS/P-2.7_35 ºC
35 ºC - 1.78
75 ºC - 2.09
CO2 Adsorbed (mmol CO2/g)
Time (min)
(b)
BS/P-2.9_75 ºC
BS/P-2.9_35 ºC
35 ºC - 1.96
75 ºC - 2.18
CO2 Adsorbed (mmol CO2/g)
Time (min)
(c)
BS/P-3.24_75 ºC
BS/P-3.24_35 ºC
35 ºC - 1.89
75 ºC - 2.22
CO2 Adsorbed (mmol CO2/g)
Time (min)
(d)
BS/P-2.7_35 ºC
BS/P-2.7_75 ºC
CO2
Pore
PEI
SiO2
CO2 Ads. Rate (mmol CO2/g*min)
Time (min)
(e)
BS/P-2.9_35 ºC
BS/P-2.9_75 ºC
CO2
Pore
PEI
SiO2
CO2 Ads.Rate (mmol CO2/g*min)
Time (min)
(f)
BS/P-3.24_35 ºC
BS/P-3.24_75 ºC
noise
CO2
Film
Pore
PEI
SiO2
CO2 Ads.Rate (mmol CO2/g*min)
Time (min)

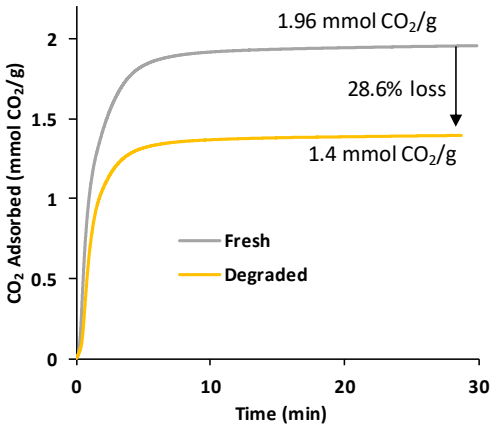
1.96 mmol CO2/g
28.6% loss
1.4 mmol CO2/g
Fresh
Degraded
CO2 Adsorbed (mmol CO2/g)
Time (min)
0
0.5
1
1.5
2
0
10
20
30

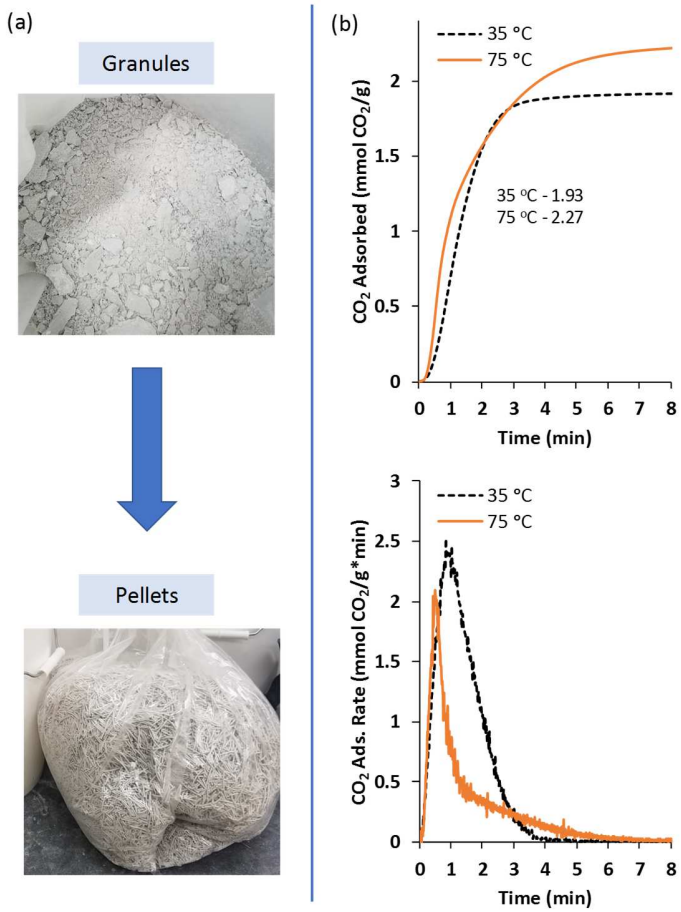
(a)
Granules
Pellets
(b)
35 °C
75 °C
35 °C - 1.93
75 °C - 2.27
CO2 Adsorbed (mmol CO2/g)
Time (min)
CO2 Ads. Rate (mmol CO2/g*min)
Time (min)

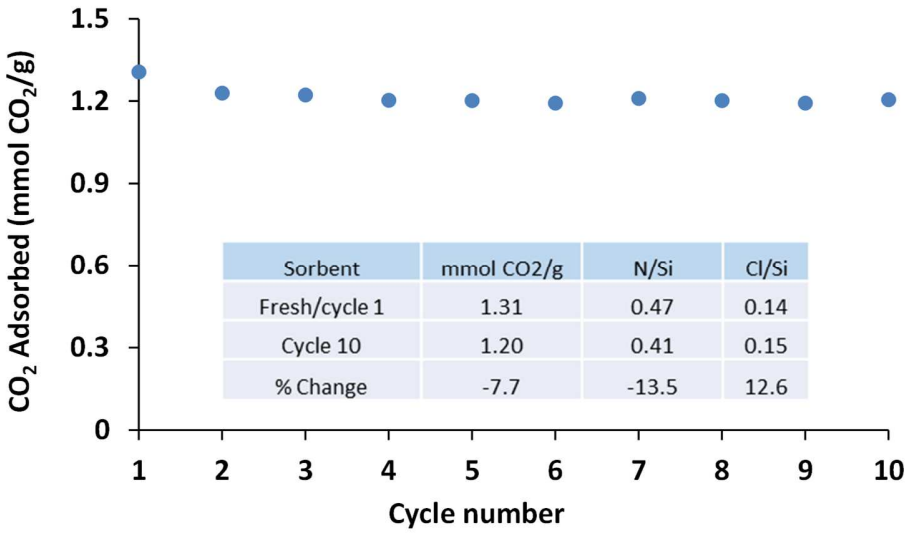

Sorbent	mmol CO2/g	N/Si	Cl/Si
Fresh/cycle 1	1.31	0.47	0.14
Cycle 10	1.20	0.41	0.15
% Change	-7.7	-13.5	12.6

Table 1: Physical properties of silica and fly ash used to prepare pellets, as determined by surface, pore, and particle size distribution analyses. Particle skeletal densities of the powders were between 2.2 and 2.4 g/cm^3.*Values were calculated from those of their pure components and their weighted ratios in the mixture.

Material	BET surface area (m^2/g)	BJH pore volume (cm^3/g)	BJH pore size, $D_{pore, avg.}$ (nm)	D_{10} (μm)	D_{50} (μm)	D_{90} (μm)
SiO_2, CS-2133 granular	365	2.5	27.5			
SiO_2,CS-2129 granular	290	2.5	34.5			
SiO_2, CS-2129 ground (GS)	289	2.1	13.4	7.6	19	43
SiO_2, CS-2129 100 μm (S_{100})	248	2.5	13.4	42.1	108	187
Fly ash (FA)	54.9	0.24	9.1	7.9	100	334
FA/GS_{2133}-10/90	341	2.6		8.3*	24.3*	60*
FA/GS_{2129}-10/90	280	2.0	13.7	7.6*	18.7*	42.0*
FA/S_{100}-10/90	232	2.4	13.7	41.2*	105.4*	182.4*

optimize
visco-elasticity

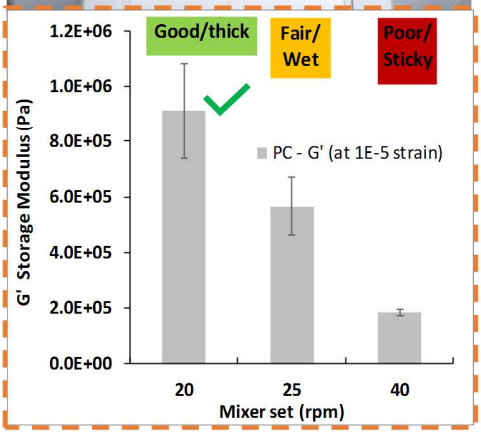

semi-pilot
trials